

Algorithms for Nonlinear Mixed-Integer Location Estimation

Ophir Uziel, Efi Fogel, Dan Halperin, and Sivan Toledo

April 2025

Abstract

For three decades, carrier-phase observations have been used to obtain the most accurate location estimates using global navigation satellite systems (GNSS). These estimates are computed by minimizing a nonlinear mixed-integer least-squares problem. Existing algorithms linearize the problem, orthogonally project it to eliminate real variables, and then solve the integer least-square problem. There is now considerable interest in developing similar localization techniques for terrestrial and indoor settings. We show that algorithms that linearize first fail in these settings and we propose several algorithms for computing the estimates. Some of our algorithms are elimination algorithms that start by eliminating the non-linear terms in the constraints; others construct a geometric arrangement that allows us to efficiently enumerate integer solutions (in polynomial time). We focus on simplified localization problems in which the measurements are range (distance) measurements and carrier phase range measurements, with no nuisance parameters. The simplified problem allows us to focus on the core question of untangling the nonlinearity and the integer nature of some parameters. We show using simulations that the new algorithms are effective at close ranges at which the linearize-first approach fails.

1 Introduction

For three decades, carrier-phase observations have been used to obtain the most accurate location estimates using global navigation satellite systems (GNSS) [16, 17, 21, 4]. While originally designed for measuring the signal’s time of arrival (ToA), which varies linearly with the range (distance) between the emitting satellite and the receiver, it turns out that the receiver can also measure and track the carrier’s phase, which also varies linearly with the range, but wraps around every whole wavelength. The errors in the phase measurements are orders of magnitude smaller than in the ToA estimates, when both are expressed in meters, allowing in principle more accurate location estimates. However, to resolve the location of the receiver from carrier-phase measurements, the receiver needs to resolve the so-called *integer ambiguities*, essentially the number of whole wavelengths between each satellite and the receiver (the actual formulation also

involves nuisance parameters such as the initial phases at the satellite and the receiver). A method called LAMBDA [16, 6] was invented to efficiently resolve the integer ambiguities, along with a few variants [21, 4, 3]. These methods work well in both single-epoch settings and in multi-epoch settings in which the receiver is either stationary or moving (in the latter setting the method is referred to as real-time kinematic positioning, or RTK).

There is now considerable interest in developing carrier-phase positioning for terrestrial localization systems, where the distances between the emitters and the receivers are much smaller than in GNSS, including in cellular and indoor systems [19, 7, 13].

Unfortunately, recent work on short-range carrier localization propose using LAMBDA and its variants, implicitly assuming that these methods are suitable for this setting [22, 19, 7].

We show in this paper that this assumption is often wrong. LAMBDA and its variants start by linearizing a nonlinear mixed-integer least-squares problem around an approximate solution. The nonlinearity is the Euclidean distance between the emitter and receiver, which is huge in GNSS. Therefore, in GNSS settings the linearization introduces essentially no error, even if the approximate solution (usually obtained from ToA measurements) is not particularly good. In terrestrial and indoor settings, where the distances between the emitters and receivers are on the order of meters or kilometers, this is no longer true; we show below that LAMBDA variants fail at these distances.

The main contributions of this paper are two families of algorithms for resolving the integer ambiguities in simplified location-estimation problems that include both range measurements and carrier-phase range measurements. Our algorithms tackle the nonlinearity head-on. One family of algorithms is based on elimination of the nonlinear terms. In one algorithm, described in Section 4, we use non-linear elimination, reminiscent of closed-form solutions for code-phase GNSS localization [1, 15]. In another algorithm from the same family, described in Section 6, we use double differencing in cases where the target is tracked over two or more epochs. A second family of algorithms, described in Section 8, uses geometric arrangements to resolve the ambiguities.

We show in simulations that our methods are both efficient and effective, and that they can resolve the integer ambiguities at ranges where LAMBDA fails due to the linearization error.

The localization problems that we resolve are simplified in the sense that they include range observations and observations of the remainders of division of the ranges by the wavelength. These problems lack nuisance parameters such as clock bias and initial phases at the emitters and receiver, parameters that are usually necessary in a realistic system model. (The lack of these nuisance parameters also mean that measurements at a reference receiver whose location is known are not necessary.)

We chose to focus on these simplified localization problems, which still retain the Euclidean nonlinearity and the mixture of real and integer parameters, to enable the widest possible exploration of the algorithmic design space. We plan to explore localization problems associated with realistic system models and to

extend our algorithms to these cases in the near future.

2 Problem Statement

We wish to localize a target at Cartesian coordinates $\ell = [x \ y \ z]^T$ from range or pseudo-range measurements from a set of reference points $\rho_i = [x_i \ y_i \ z_i]^T$, as well as carrier-phase measurements from the same reference points. The simplest setting for such problems is:

$$r_i = \|\ell - \rho_i\|_2 + \epsilon_i \tag{1}$$

$$\lambda\varphi_i + \lambda n_i = \|\ell - \rho_i\|_2 + \delta_i, \tag{2}$$

where r_i is a noisy range (distance) measurement, ϵ_i is the range-measurement error (noise), λ is the wavelength of the carrier wave of the signal emitted by the references (or by the target, in transmitter localization), $n_i = \lfloor \|\ell - \rho_i\| / \lambda \rfloor \in \mathbb{N}$, $\varphi_i \in [0, 1)$ is a noisy phase measurement, and δ_i is the phase measurement error. In more realistic problems only pseudo-ranges are measured $\|\ell - \rho_i\| + c\Delta t$ where Δt is a clock error or bias and c is the speed of propagation) and the phases are measured relative to some unknown initial phase at both the transmitter and the receiver. There might also be complications from ionospheric delays, tropospheric delays, etc.

These problems are interesting when $\delta_i \ll \epsilon_i$. Typical value of λ for radio systems range from about 1 m to about 10 cm, typical standard deviations for ϵ_i are on the scale of 10 m, and typical standard deviations for δ_i are on the scale of $\lambda/100$, so about 1 cm to 1 mm.

We wish to estimate ℓ in the generalized least-squares sense, which corresponds to maximum likelihood under the assumptions that ϵ_i and δ_i are unbiased Gaussian random variables. We further assume that the ϵ_i and δ_i are uncorrelated and have known standard deviations. Under these assumptions, we seek the minimizer

$$\arg \min_{\ell, n} \left\| W \left(M(\ell) - \begin{bmatrix} 0 \\ \lambda I \end{bmatrix} n - \begin{bmatrix} r_i \\ \lambda\varphi_i \end{bmatrix} \right) \right\|_2$$

where W is a diagonal matrix with $\sigma^{-1}(\epsilon_i)$ and $\sigma^{-1}(\delta_i)$ on the diagonal, and M is a function such that

$$\begin{aligned} M_i(\ell) &= \|\ell - \rho_i\|_2 \\ M_{m+i}(\ell) &= \|\ell - \rho_i\|_2. \end{aligned}$$

In GNSS, we can obtain a coarse estimate ℓ_0 of ℓ from the (pseudo) range measurements alone, and then linearize M around ℓ_0 ,

$$M(\ell) \approx M(\ell_0) + J_M(\ell - \ell_0) = M(\ell_0) + \frac{\partial M}{\partial \ell}(\ell - \ell_0)$$

where $J_M = \frac{\partial M}{\partial \ell}$ is the Jacobian of M , and where the derivatives are evaluated at ℓ_0 . In GNSS, the distances $\|\ell - \rho_i\|$ are 20,000 km or more, so when ℓ_0 is

within tens or even hundreds of meters of ℓ , this linear approximation is superb, so the carrier phases can be used effectively by solving the mixed-integer least-squares problem

$$\arg \min_{\Delta\ell, n} \left\| W \left(M(\ell_0) + J_M \Delta\ell - \begin{bmatrix} 0 \\ \lambda I \end{bmatrix} n - \begin{bmatrix} r_i \\ \lambda \varphi_i \end{bmatrix} \right) \right\|_2. \quad (3)$$

Note that the same W appears in this expression, because the linearization errors at GNSS ranges are so small that their effect on the overall errors is completely insignificant.

We are interested in problems in which the ranges are much smaller, so that the linear approximation is no longer good enough. In other words, in GNSS a reasonably good ℓ_0 allows us to ignore the nonlinearity in M . The only difficulty is the estimation of the integer ambiguities. This is true even if there are additional nuisance parameters like clock bias, because the dependence on them is linear.

We are interested in cases in which the nonlinearity of M cannot be ignored due to much shorter ranges $\|\ell - \rho_i\|$.

3 Parameters for Experimental Evaluations

We use parameter values that are typical of GNSS, except for the distances to the references. More specifically, our baseline values are

$$\begin{aligned} \lambda &= 19 \text{ cm} \\ \sigma(\epsilon_i) &= 10 \text{ m} \\ \sigma(\delta_i) &= 0.1^\circ = 19/3600 \text{ cm} \\ \sigma |\ell - \ell_0|_j &= 10 \text{ m} \\ \|\ell - \rho_i\| &\approx 10 \text{ m to } 20,000 \text{ km} \end{aligned}$$

We test the algorithms in 2D, and 3D. We select $\ell - \ell_0$ at random from a Gaussian distribution of each coordinate. We select the ρ_i s by selecting a uniform random azimuth from ℓ , selecting a point on a circular orbit at that azimuth, and then perturbing the coordinates by adding random Gaussian noise to each coordinate of ρ_i . The standard deviation of these perturbations is 10% of the nominal range.

4 A Square-and-Difference Approach

The problem (3) minimizes the 2-norm of an affine function of both a real vector $\Delta\ell$ and an integer vector n . The standard solution approach for such problems, often referred to as LAMBDA [5, 16, 17, 21], solves the problem in four steps:

1. The affine function is projected orthogonally to the subspace orthogonal to the column space of WJ_M , which eliminates the real parameters $\Delta\ell$.

This also transforms the matrix that n is multiplied by and the known vector.

2. The matrix that now multiplies n is factored into a product of an orthonormal matrix Q and a square upper-triangular matrix R , and Q^T is applied to the function that we minimize. This transforms again the known vector, and R replaces the matrix that n is multiplied by.
3. The LLL algorithm or one of its variants [10, 12, 11] is applied to R in an attempt to improve the performance of the next step. This step multiplies R from the right by a series of unimodular transformations that maintain its upper-triangular form. The use of unimodular transformations ensures that the integer minimizer of the LLL-transformed problem can be transformed back into an integer vector.
4. The Schnorr-Euchner search algorithm [14] finds the integer minimizer of the upper-triangular transformed problem. This algorithm is a specialized branch-and-bound exhaustive search with a superficial similarity to back substitution.

We note that only step 3 and 4 are specific to the integers. Step 1 is very general and can be used to eliminate real parameters that a least-squares residual depends on linearly. It is often used to reduce the dimension of non-linear least-squares problems. Step 2 is also quite general; it can be applied to any linear least-squares problem, whether the parameters are real, integers, or any other set. Steps 3 and 4 are specific to integers.

However, we discovered that step 4 can be easily adapted to vectors of discrete parameters, even if the discrete set of values that each parameter can take is not the set of integers.

We exploit this insight, together with the assumption that the errors δ_i of the phase measurements are tiny, to transform our constraints into a least-squares minimization of an affine function of a real vector and a vector of discrete parameters (which are not integers). Our technique, which we call the *square-and-difference* approach, is based on ideas from closed-form solvers for GNSS constraints [1, 15].

4.1 Squaring and Differencing

We start with the carrier-phase measurement equation for satellite i ,

$$\lambda(n_i + \varphi_i) = \|\ell - \rho_i\|_2 + \delta_i. \quad (4)$$

We square both sides,

$$\lambda^2(n_i + \varphi_i)^2 = \|\ell - \rho_i\|_2^2 + 2\delta_i \|\ell - \rho_i\|_2 + \delta_i^2. \quad (5)$$

We assume that the covariance matrix of the δ_i s is diagonal with diagonal elements $\sigma^2(\delta_i)$. We replace the error terms in Equation (5) with approximations

that ignore the tiny δ_i^2 s,

$$\lambda^2 (n_i + \varphi_i)^2 \approx \|\ell - \rho_i\|_2^2 + \Delta_i \quad (6)$$

where $\Delta_i = 2\delta_i\|\ell - \rho_i\|$. The covariance matrix of these approximate constraints is still diagonal with diagonal elements $4\sigma^2(\delta_i)\|\ell - \rho_i\|_2^2$.

We now choose one of the satellites, say 1, and subtract its squared equation from the rest,

$$\lambda^2 \left((n_i + \varphi_i)^2 - (n_1 + \varphi_1)^2 \right) \approx \|\ell - \rho_i\|_2^2 - \|\ell - \rho_1\|_2^2 + \Delta_i - \Delta_1. \quad (7)$$

Expanding the squared norms on the right-hand side gives

$$\begin{aligned} \|\ell - \rho_i\|_2^2 - \|\ell - \rho_1\|_2^2 &= (\ell - \rho_i)^T(\ell - \rho_i) - (\ell - \rho_1)^T(\ell - \rho_1) \\ &= -2\ell^T(\rho_i - \rho_1) + \rho_i^T \rho_i - \rho_1^T \rho_1. \end{aligned} \quad (8)$$

The subtraction eliminated the squares $\ell^T \ell = x^2 + y^2 + z^2$, leaving us with a linear expression.

We define a vector s of discrete variables of the form

$$s_i = (n_i + \varphi_i)^2 \text{ where } n_i \in \mathbb{N}$$

where φ_i is a known constant. We rewrite our constraints as

$$\lambda^2 s_i - \lambda^2 s_1 \approx -2\ell^T(\rho_i - \rho_1) + \rho_i^T \rho_i - \rho_1^T \rho_1 + \Delta_i - \Delta_1$$

or

$$\lambda^2 s_i - \lambda^2 s_1 + 2\ell^T(\rho_i - \rho_1) - (\rho_i^T \rho_i - \rho_1^T \rho_1) \approx \Delta_i - \Delta_1.$$

We also derive an expression of the same form from the carrier-phase constraint for satellite 1, the constraint that we subtract from the others. We start from Equation (6),

$$\lambda^2 (n_1 + \varphi_1)^2 \approx \|\ell - \rho_1\|_2^2 + \Delta_1$$

and we expand $\|\ell - \rho_1\|$ around $\ell_0 = [x_0 \ y_0 \ z_0]^T$, the estimate obtained from the code-phase constraints,

$$\|\ell - \rho_1\|_2^2 = \|\ell - \ell_0 + \ell_0 - \rho_1\|_2^2 = \|\ell_0 - \rho_1\|_2^2 + 2(\ell_0 - \rho_1)^T(\ell - \ell_0) + \|\ell - \ell_0\|_2^2.$$

We drop the nonlinear term $\|\ell - \ell_0\|^2$ and treat it as a random error ξ with a known standard deviation, the expected error in ℓ_0 squared. This gives us a constraint

$$\lambda^2 s_1 \approx \|\ell_0 - \rho_1\|_2^2 + 2(\ell_0 - \rho_1)^T(\ell - \ell_0) + \Delta_1 + \xi$$

or

$$\lambda^2 s_1 - 2\ell^T(\ell_0 - \rho_1) + 2\ell_0^T(\ell_0 - \rho_1) - \|\ell_0 - \rho_1\|_2^2 \approx \Delta_1 + \xi.$$

The constant term can be simplified a bit:

$$\begin{aligned}
2\ell_0^T(\ell_0 - \rho_1) - \|\ell_0 - \rho_1\|_2^2 &= 2x_0(x_0 - x_1) - (x_0 - x_1)^2 + \dots \\
&= (2x_0 - x_0 + x_1)(x_0 - x_1) + \dots \\
&= (x_0 + x_1)(x_0 - x_1) + \dots \\
&= x_0^2 - x_1^2 + \dots
\end{aligned}$$

(showing only the x terms).

We define a least-squares minimization of these constraints

$$\hat{\ell}, \hat{s} = \arg \min_{\ell, s} \|W(A\ell + Bs - d)\|_2 \quad (9)$$

where

$$A = \begin{bmatrix} 2(x_1 - x_0) & 2(y_1 - y_0) & 2(z_1 - z_0) \\ 2(x_2 - x_1) & 2(y_2 - y_1) & 2(z_2 - z_1) \\ 2(x_3 - x_1) & 2(y_3 - y_1) & 2(z_3 - z_1) \\ \vdots & \vdots & \vdots \\ 2(x_m - x_1) & 2(y_m - y_1) & 2(z_m - z_1) \end{bmatrix} \quad \text{and} \quad B = \lambda^2 \begin{bmatrix} 1 & & & & \\ -1 & 1 & & & \\ -1 & & 1 & & \\ \vdots & \vdots & \vdots & \ddots & \\ -1 & & & & 1 \end{bmatrix},$$

and

$$d = \begin{bmatrix} x_1^2 + y_1^2 + z_1^2 - x_0^2 - y_0^2 - z_0^2 \\ x_2^2 + y_2^2 + z_2^2 - x_1^2 - y_1^2 - z_1^2 \\ x_3^2 + y_3^2 + z_3^2 - x_1^2 - y_1^2 - z_1^2 \\ \vdots \\ x_m^2 + y_m^2 + z_m^2 - x_1^2 - y_1^2 - z_1^2 \end{bmatrix}.$$

The matrix $B \in \mathbb{R}^{m \times m}$ has full rank. The weigh matrix W is an inverse factor $W^T W = C^{-1}$ of the covariance matrix C of the error terms

$$\begin{bmatrix} \Delta_1 + \xi \\ \Delta_2 - \Delta_1 \\ \Delta_3 - \Delta_1 \\ \vdots \\ \Delta_m - \Delta_1 \end{bmatrix} = \begin{bmatrix} 1 & & & & 1 \\ -1 & 1 & & & \\ -1 & & 1 & & \\ \vdots & \vdots & \vdots & \ddots & \\ -1 & & & & 1 \end{bmatrix} \begin{bmatrix} \Delta_1 \\ \Delta_2 \\ \vdots \\ \Delta_m \\ \xi \end{bmatrix}.$$

We assume that the δ_i s are uncorrelated and we approximate here $\|\ell - \rho_i\|$ by $\|\ell_0 - \rho_i\|$, which gives good enough weights. This implies that the approximations $2\delta_i\|\ell_0 - \rho_i\|$ of Δ_i are uncorrelated. We also approximate the error $\xi = \|\ell - \ell_0\|^2$ by the square of the expectation of the error $\|\ell - \ell_0\|^2$, which is again uncorrelated with the δ_i s and hence with our approximation of the Δ_i s.

so where

$$C = \begin{bmatrix} 1 & & & & 1 \\ -1 & 1 & & & \\ -1 & & 1 & & \\ \vdots & \vdots & \vdots & \ddots & \\ -1 & & & & 1 \end{bmatrix} \text{diag} \left(\begin{bmatrix} 4\sigma^2(\delta_1)\|\ell_0 - \rho_1\|^2 \\ 4\sigma^2(\delta_2)\|\ell_0 - \rho_2\|^2 \\ \vdots \\ 4\sigma^2(\delta_m)\|\ell_0 - \rho_m\|^2 \\ \text{expectation}^2(\|\ell - \ell_0\|^2) \end{bmatrix} \right) \begin{bmatrix} 1 & & & & 1 \\ -1 & 1 & & & \\ -1 & & 1 & & \\ \vdots & \vdots & \vdots & \ddots & \\ -1 & & & & 1 \end{bmatrix}^T$$

In summary, the C matrix that the algorithm constructs is based on three approximations: ignoring the δ_i^2 terms, the approximate ranges $\|\ell_0 - \rho_i\|$, and the approximate error $\|\ell - \ell_0\|$.

We form W by computing a Cholesky factorization $C = LL^T$ with L lower triangular and setting $W = L^{-1}$. To multiply a matrix Y , say, by W we solve a triangular linear system $LX = Y$ to obtain $X = L^{-1}Y$. This avoids the explicit inversion of L .

4.2 Incorporating Range Constraints

Up to now we ignored the noisy but unambiguous range constraints $r_i = \|\ell - \rho_i\|_2 + \epsilon_i$. We can use them in three ways. First, we can try to linearize these constraints around some ℓ_0 , say the least-squares solution of these constraints alone and to add these linearized constraints to (9), with weights

$$(\text{var}(\epsilon_i) + \text{var}(\ell - \ell_0))^{-1/2} .$$

Second, we can apply the square-and-difference technique to the constraints $r_i = \|\ell - \rho_i\|_2 + \epsilon_i$ and add this linearization to (9), again properly weighted. The derivation of the weights is virtually identical to the derivation above.

In the experiments below, we use both the first and second constraints, appropriately weighted.

We can also use the range constraints to constrain the range of n_i s. For example, if we assume that the ϵ_i s are Gaussian, we can limit the search to 6 standard deviations. In other words, these constraints tell us that values outside some range of integers are highly unlikely for n_i . We do not use these constraints in our implementation, but it might be a useful tool in other algorithmic variants.

We now combine the squared-and-differenced phase constraints with linear constraints on ℓ derived from range observations (two constraints for each observation) to form a system with more constraints, denoted

$$\hat{\ell}, \hat{s} = \arg \min_{\ell, s} \|\bar{W}(\bar{A}\ell + \bar{B}s - \bar{d})\|_2 . \quad (10)$$

4.3 Eliminating the Real Parameters

We use an orthogonal projection to eliminate ℓ from this combined system. Let $U \in \mathbb{R}^{m \times 3}$ be an orthonormal basis for the column space of $\bar{W}\bar{A}$, obtained from a QR factorization or the SVD. We project the minimization problem (9) onto the complementary subspace,

$$\begin{aligned} \hat{s} &= \arg \min_{\ell, s} \|\bar{W}(\bar{A}\ell + \bar{B}s - \bar{d})\|_2 \\ &= \arg \min_s \|(I - UU^T)(\bar{B}s - \bar{d})\|_2 . \end{aligned}$$

Once we recover \hat{s} from this expression, we can recover $\hat{\ell}$ using a least-squares solver over \mathbb{R}^3 . The recovery of \hat{s} is done using a QR factorization of $(I - UU^T)\bar{B}$ and a modified Schnorr-Euchner search. We describe these steps below.

5 Solving the Square-and-Difference Minimization Problem

We now show how to solve the reduced least-squares minimization problem, in which all the parameters are discrete.

5.1 Adapting the Schnorr-Euchner Search to Shifted Squares

We now show how to solve a problem of the form

$$\hat{s} = \arg \min_s \|(I - UU^T)(Bs - d)\|_2, \quad s_i = (n_i + \varphi_i)^2 \text{ where } n_i \in \mathbb{N}$$

using an adaption of the Schnorr-Euchner search. We first compute the QR factorization of $(I - UU^T)B = QR$, where $Q \in \mathbb{R}^{m \times m}$ is unitary and $R \in \mathbb{R}^{m \times m}$ is upper triangular,

$$\begin{aligned} \hat{s} &= \arg \min_s \|(I - UU^T)(Bs - d)\|_2 \\ &= \arg \min_s \|Rs - Q^T d\|_2. \end{aligned}$$

Adapting the Schnorr-Euchner Search

We now run the Schnorr-Euchner search algorithm, except that the set of values $n_{i,k}$ that we substitute for n_i are not integers but rather numbers of the form $(n_{i,k} + \varphi_i)^2$ where $n_{i,k} \in \mathbb{N}$. Also, when the values of n_m, \dots, n_{i+1} are fixed, the contribution of row i to the sum of squares is

$$(R_{i,i}s_i + R_{i,i+1:m}s_{i+1:m} - (Q^T d)_i)^2, \quad (11)$$

where $s_j = (n_j + \varphi_j)^2$. For the Schnorr-Euchner search to work when we constrain s_i to the set $(n_i + \varphi_i)^2$, $n_i \in \mathbb{N}$, we must enumerate candidate values such that (11) increases monotonically. We denote

$$z_i = -\frac{R_{i,i+1:m}s_{i+1:m} - (Q^T d)_i}{R_{i,i}}.$$

The contribution of row i is

$$\left((n_i + \varphi_i)^2 - z_i \right)^2.$$

The square root is monotone, so this expression is minimized when $|(n_i + \varphi_i)^2 - z_i|$ is minimized. We test both $\lfloor \sqrt{z_i} - \varphi_i \rfloor$ and $\lceil \sqrt{z_i} - \varphi_i \rceil$ and assign to $n_{i,1}$ the value n_1 that yields the smaller contribution. This is the equivalent of Babai rounding for this problem. Now suppose that we tested integer values $n_1 - l$ to $n_1 + r$. The next largest contribution will be either at $n_1 - l - 1$ or $n_1 + r + 1$. We again test both and take the one that yields the smaller contribution.

We note that this adaptation is valid for any set of discrete values that we can enumerate in increasing distance from a real value z_i .

5.2 Custom QR Decomposition with Increasing Pivoting

In integer least squares problems, lattice basis reduction techniques like the LLL algorithm are often used to improve the efficiency of the Schnorr-Euchner search. More specifically, these algorithms replace the upper triangular R into RG , which is still upper triangular and where G is unimodular. Therefore, for any integer vector n we have $Rn = RGG^{-1}n = (RG)(G^{-1}n)$, where $G^{-1}n$ is also an integer vector. Therefore, we can carry out the search on RG and then transform its minimizer $G^{-1}n$ back into the minimizer n associated with R .

We apply the Schnorr-Euchner search to sets of shifted squares, so we need G to preserve this property. Unimodular matrices do not necessarily preserve this property. Therefore, we utilize a more restricted class of matrices, namely permutation matrices.

The aim of the transformation of R is to populate the diagonal of RG with large entries near the bottom, which translate unit increments in the corresponding integer to large increments in the sum of squares. This causes more rapid pruning the Schnorr-Euchner search.

To achieve a similar effect, we incorporate column pivoting into the QR factorization that produces R . The pivoting selects the column with the smallest norm to be eliminated next. This is the exact opposite of the policy of column pivoting in numerical libraries, which has a different aim, to identify rank deficiency.

We report below on the efficacy of this optimization.

6 Double Differencing for Real-Time Kinematic Localization

6.1 Squaring and Double Differencing to Form a Mixed-Integer Linear Least-Squares Problem

Up to now we assumed that all the measurements are from one epoch, one measurement per satellite. If we track the carrier phase continuously over several epochs we obtain multiple constraints per satellite, of the form

$$\begin{aligned} \lambda\varphi_{i,1} + \lambda n_i &= \|\ell_1 - \rho_{i,1}\|_2 + \delta_{i,1} \\ \lambda\varphi_{i,2} + \lambda n_i &= \|\ell_2 - \rho_{i,2}\|_2 + \delta_{i,2} \\ &\vdots \end{aligned}$$

All of the constraints for satellite i use a single integer unknown, n_i . In principle, the more epochs we collect, the easier it should be to estimate the n_i s.

One approach is to perform the squaring and differencing as described in Section 4. For each epoch we now have the set of constraints from Equation 9, which we reproduce here with epoch indices:

$$\hat{\ell}_j, \hat{s}_j = \arg \min_{\ell, s} \|W_j (A_j \ell_j + B s_j - d_j)\|_2 . \quad (12)$$

Note that B depends only λ , not on the locations $\rho_{i,j}$ of the satellites. The matrix A and the vector d are functions of the $\rho_{i,j}$ s.

We now expand the s_j s,

$$s_{i,j} = (\varphi_{i,j} + n_i)^2 = \varphi_{i,j}^2 + 2\varphi_{i,j}n_i + n_i^2 .$$

If we subtract the residual $A_j \ell_j + B_j s_j - d_j$ for epoch j from the residual for epoch j' , the n_i^2 terms drop from the doubly-differenced constraints. We have

$$\begin{aligned} (A_j \ell_j + B s_j - d_j) - (A_{j'} \ell_{j'} + B s_{j'} - d_{j'}) &= (A_j \ell_j - A_{j'} \ell_{j'}) + (B s_j - B s_{j'}) - (d_j - d_{j'}) \\ &= (A_j \ell_j - A_{j'} \ell_{j'}) + B (s_j - s_{j'}) - (d_j - d_{j'}) . \end{aligned}$$

The elements of the difference of the s_j s is

$$\begin{aligned} s_{i,j} - s_{i,j'} &= (\varphi_{i,j}^2 + 2\varphi_{i,j}n_i + n_i^2) - (\varphi_{i,j'}^2 + 2\varphi_{i,j'}n_i + n_i^2) \\ &= (\varphi_{i,j}^2 - \varphi_{i,j'}^2) + 2(\varphi_{i,j} - \varphi_{i,j'})n_i . \end{aligned}$$

This expression is linear in n_i , meaning we should be able to use LLL and the original Schorr-Euchner search. But first we need to address the rest of the terms of the constraints and their weights. In the general case in which both the satellites and the target move, so $\rho_{i,j} \neq \rho_{i,j'}$ and $\ell_j \neq \ell_{j'}$, the doubly-differenced constraints are

$$\hat{\ell}_j, \hat{\ell}_{j'}, \hat{n} = \arg \min_{\ell_j, \ell_{j'}, s} \|W_{j,j'} (A_j \ell_j - A_{j'} \ell_{j'} + C n_i + B \phi_{j,j'} - d_j + d_{j'})\|_2 , \quad (13)$$

where $\phi_{j,j'}$ denote the vector whose elements are $\varphi_{i,j}^2 - \varphi_{i,j'}^2$, where

$$C = 2B \begin{bmatrix} \varphi_{1,j} - \varphi_{1,j'} & & & & \\ & \varphi_{2,j} - \varphi_{2,j'} & & & \\ & & \ddots & & \\ & & & \ddots & \\ & & & & \varphi_{m,j} - \varphi_{m,j'} \end{bmatrix} ,$$

and where $W_{j,j'}$ is the appropriate weight matrix.

Some special cases deserve additional attention. If the target remains stationary so $\ell_j = \ell_{j'} = \ell$, the constraints simplify to

$$\hat{\ell}, \hat{n} = \arg \min_{\ell, n} \|W_{j,j'} ((A_j - A_{j'}) \ell + C n_i + B \phi_{j,j'} - d_j + d_{j'})\|_2 . \quad (14)$$

If the target moves but the satellites do not, we get another special case,

$$\hat{\ell}_j, \hat{\ell}_{j'}, \hat{n} = \arg \min_{\ell_j, \ell_{j'}, n} \|W_{j,j'} (A (\ell_j - \ell_{j'}) + C n_i + B \phi_{j,j'} - d_j + d_{j'})\|_2 . \quad (15)$$

This does not resolve the absolute locations, which must now be resolved by substituting the optimal \hat{n} in the original constraints. If both the target and the satellites are stationary, the location terms drop entirely and we have

$$\hat{n} = \arg \min_n \|W_{j,j'} (Cn_i + B\phi_{j,j'} - d_j + d_{j'})\|_2 . \quad (16)$$

We again have to resolve the location in a separate step.

The weight matrix $W_{j,j'}$ of the differenced constraints is the inverse of the Cholesky factor of $C_j + C_{j'}$.

6.2 Incorporating Linearized Constraints

We can also linearize the range expressions in the phase observations

$$\begin{aligned} \lambda\varphi_{i,1} + \lambda n_i &= \|\ell_1 - \rho_{i,1}\|_2 + \delta_{i,1} \\ \lambda\varphi_{i,2} + \lambda n_i &= \|\ell_2 - \rho_{i,2}\|_2 + \delta_{i,2} \\ &\vdots \end{aligned}$$

around solutions of the range constraints alone, $\ell_{0,1}$ and $\ell_{0,2}$. This generates another set of linear least-squares mixed-integer constraints, but with much larger errors and hence much smaller weights,

$$(\text{var}(\delta_{i,j}) + f(\sigma\|\ell - \ell_{0,j}\|, \ell_{0,j} - \rho_{i,j}))^{-1/2} ,$$

where f is an approximation of the variance of the linearization error. We discuss this approximation below. We add these constraints to the least-squares system. Note that in each such constraint the parameters are ℓ_1 or ℓ_2 (and possibly more if there are more than 2 epochs) and n_i , the same as in the squared and double-differenced constraints (which tend to have much smaller errors).

Note that we could not use these constraints in the single-differencing approach presented in Section 4, since the discrete parameters in that approach are not the n_i s.

6.3 Incorporating Range Constraints

As in Section 4, we now add constraints derived from the range observations

$$r_{i,j} = \|\ell_j - \rho_{i,j}\|_2 + \epsilon_{i,j} .$$

We again use each range constraint twice. First, we use the squaring and double-differencing technique of Section 6.1 to form a set of linear least-squares constraints with real parameters, ℓ_1 and ℓ_2 (possibly more if there are more than 2 epochs). Second, we linearize the range constraints of each epoch around an approximate solution $\ell_{0,1}$ and $\ell_{0,2}$, forming a set of linear least-squares constraints with real parameters. The weights that we assign are derived in a similar way to those used in the previous section.

7 Weighing Constraints with Linearization Errors

When the ranges $\|\ell - \rho_i\|$ are small, linearization of the range expressions introduces significant errors. When linearized expressions form constraints, the weight of these constraints depends on the scale of the linearization errors. We present a partial analysis of these errors and we explain how we weigh them. These weights affect the performance of a modified LAMBDA approach, in which we use these weights (as explained above, LAMBDA methods normally ignore the linearization errors, which are insignificant at GNSS ranges) and the performance of the squaring and double-differencing approach (Section 6.1).

It is not difficult to show that in the linearization of $E_i(\ell) = \|\ell - \rho_i\|_2$

$$M(\ell) \approx M(\ell_0) + J_M(\ell - \ell_0) ,$$

the elements of the Jacobian are

$$\begin{aligned} J_{M_i}(\ell - \ell_0) &= \frac{(\ell_0 - \rho_i)^T}{\|\ell_0 - \rho_i\|_2} (\ell - \ell_0) \\ &= \|\ell - \ell_0\|_2 \frac{(\ell_0 - \rho_i)^T}{\|\ell_0 - \rho_i\|_2} \frac{(\ell - \ell_0)}{\|\ell - \ell_0\|_2} \\ &= \|\ell - \ell_0\|_2 \cos \alpha \end{aligned}$$

where $\pi - \alpha$ is the angle between the line segments $\ell_0 \leftrightarrow \ell$ and $\ell_0 \leftrightarrow \rho_i$. When ρ_i , ℓ_0 , and ℓ are collinear, the approximation is exact; either $\alpha = 0$ and $\cos \alpha = 1$ and

$$\|\ell - \rho_i\|_2 = \|\ell_0 - \rho_i\|_2 + \|\ell - \ell_0\|_2 ,$$

or $\alpha = \pi$ and $\cos \alpha = -1$ and

$$\|\ell - \rho_i\|_2 = \|\ell_0 - \rho_i\|_2 - \|\ell - \ell_0\|_2 .$$

The error is largest when $\alpha = \pi/2$ and $\cos \alpha = 0$, so the approximation is $\|\ell_0 - \rho_i\|_2$ with no correction. The magnitude of the linearization error in this case is

$$\|\ell - \rho_i\|_2 - \|\ell_0 - \rho_i\|_2 ,$$

the difference between the hypotenuse of the right triangle $\rho_i \leftrightarrow \ell_0 \leftrightarrow \ell$ and the leg $\rho_i \leftrightarrow \ell_0$ of that triangle. If we denote the long leg of the triangle $r = \|\ell_0 - \rho_i\|$ and the short leg $d = \|\ell - \ell_0\|$, the error is

$$\sqrt{r^2 + d^2} - r .$$

We now estimate the magnitude of this expression for d much smaller than

r by linearizing it at r , treating d as a perturbation. We have

$$\begin{aligned}
\sqrt{r^2 + d^2} - r &\approx (\sqrt{r^2} - r) + \frac{\partial}{\partial d} (\sqrt{r^2 + d^2} - r) d \\
&= 0 + \left(\frac{d}{\sqrt{r^2 + d^2}} \right) d \\
&= \frac{\|\ell - \ell_0\|^2}{\sqrt{r^2 + d^2}} \\
&\approx \frac{\|\ell - \ell_0\|^2}{\|\ell_0 - \rho_i\|}.
\end{aligned}$$

We define $f(d) = \sqrt{r^2 + d^2}$ and differentiate

$$\begin{aligned}
\frac{\partial f}{\partial d} &= \frac{d}{\sqrt{r^2 + d^2}} \\
\frac{\partial^2 f}{\partial d^2} &= \frac{r^2}{(r^2 + d^2)^{3/2}}.
\end{aligned}$$

We now approximate f for d close to zero (relative to a large r)

$$\begin{aligned}
f(d) &= \sqrt{r^2 + d^2} \\
&= f(0) + \frac{\partial f}{\partial d} d + \frac{1}{2} \frac{\partial^2 f}{\partial d^2} d^2 + O(d^3) \\
&\approx f(0) + \frac{\partial f}{\partial d} d + \frac{1}{2} \frac{\partial^2 f}{\partial d^2} d^2 \\
&= r + \frac{0}{r} d + \frac{1}{2} \frac{1}{r} d^2 \\
&= r + \frac{1}{2} \frac{d^2}{r}.
\end{aligned}$$

This shows that the linear approximation error, for a large range r and a small displacement d , behaves like

$$\frac{1}{2} \frac{d^2}{r}.$$

In our case, d is a random variable, so the error is also a random variable. We note that the error is always positive but we do not attempt to fully characterize its distribution. Figure 1 presents the statistics of the linearization errors for three different distributions of $\ell - \ell_0$.

In our algorithms, we weigh linearized constraints as if the linearization error was Gaussian with variance

$$f(\sigma \|\ell - \ell_0\|, \ell_0 - \rho_i) = \frac{1}{30} \frac{\|\ell - \ell_0\|^2}{\|\ell_0 - \rho_i\|}.$$

We determined the $1/30$ constant empirically, so as to give the best results we could obtain.

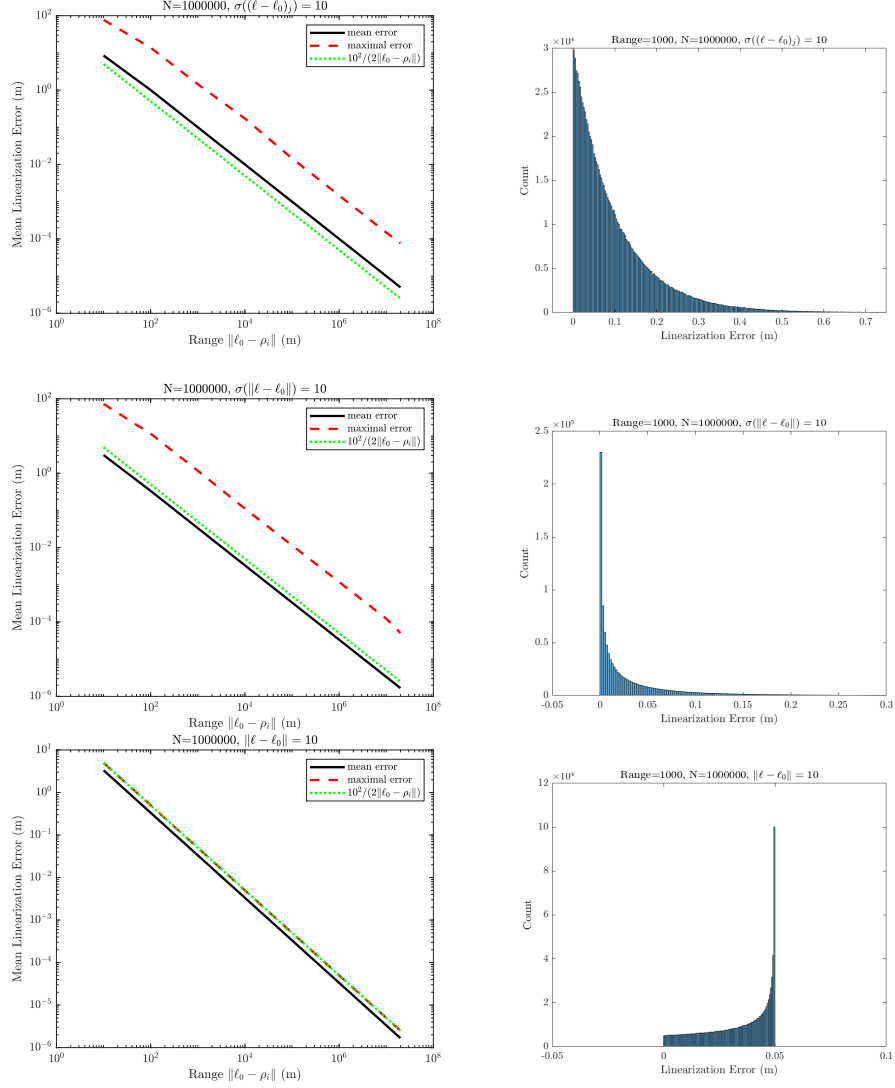


Figure 1: The distribution and mean of linearization errors for three different distributions of $\ell - \ell_0$. The top row shows the mean and maximum error as a function of the range $\|\ell_0 - \rho_i\|$, as well as a histogram of the errors at a range of 1000 m, when each coordinate of $\ell - \ell_0$ is distributed normally with zero mean and a standard deviation of 10 m. The middle row shows the same statistics when the angle between $\ell_0 - \rho_i$ and $\ell - \ell_0$ is random and uniform and $\|\ell - \ell_0\|$ is Gaussian with a zero mean and standard deviation of 10 m. The bottom row shows the statistics for a random angle and a fixed distance $\|\ell - \ell_0\| = 10$ m. The graphs also show the theoretical maximum error for a distance $\|\ell - \ell_0\| = 10$ m.

8 Brute-Force Polynomial-Time Approaches

This section describes brute-force methods that run in polynomial time. We focus on single-epoch problems for simplicity. The discussion focuses on the phase observations in Equation (2)

$$\lambda\varphi_i + \lambda n_i = \left\| \hat{\ell} - \rho_i \right\|_2 + \delta_i$$

with φ_i normalized such that $0 \leq \varphi_i < 1$. We use the range observations in equation (1)

$$r_i = \left\| \hat{\ell} - \rho_i \right\|_2 + \epsilon_i$$

to derive a probabilistic upper and lower bounds on n_i ,

$$\begin{aligned} \bar{n}_i &= \left\lceil \frac{\left\| \hat{\ell} - \rho_i \right\|_2 + c\sigma(\epsilon_i)}{\lambda} \right\rceil \\ \underline{n}_i &= \left\lfloor \frac{\left\| \hat{\ell} - \rho_i \right\|_2 - c\sigma(\epsilon_i)}{\lambda} \right\rfloor \end{aligned}$$

for some appropriate constant c , say 6. We denote by $E_i = \max_i \{\bar{n}_i - \underline{n}_i + 1\}$ an upper bound on the number of possible integers for n_i and by $E = \max_i E_i$.

We derive similar bounds on the largest plausible phase error, denoted $D_i = c\sigma(\delta_i)$, again for some appropriate c , say 6.

The general idea in these brute-force approaches is to find the minimizer of the least-squares problem

$$\hat{\ell}, \hat{n} = \arg \min_{\ell, n} \left\| W \left(M(\ell) - \begin{bmatrix} 0 \\ \lambda I \end{bmatrix} n - \begin{bmatrix} r_i \\ \lambda\varphi_i \end{bmatrix} \right) \right\|_2$$

by enumerating a set of integer vectors $\{n\}$ that contains the minimizer \hat{n} . For each enumerated integer vector n , we solve for

$$\hat{\ell}(n) = \arg \min_{\ell} \left\| W \left(M(\ell) - \begin{bmatrix} 0 \\ \lambda I \end{bmatrix} n - \begin{bmatrix} r_i \\ \lambda\varphi_i \end{bmatrix} \right) \right\|_2$$

using a continuous least-squares method such as Levenberg-Marquardt [2]. We then pick the integer vector that yielded the minimal residual in the continuous problem, as shown in Algorithm 1.

A naive way to enumerate a set of integer vectors that contain the minimizer \hat{n} is to enumerate all the integer vectors for which each $n_i \in [\bar{n}_i, \underline{n}_i]$. This set contains roughly E^m integer vectors. The next sections show that the number of integer vectors that we need to enumerate is only $O((mE)^2)$ in two dimensions and $O((mE)^3)$ in 3, and under fairly reasonable assumptions, even less, $O(E^2)$ or $O(E^3)$, respectively. In all cases, the enumeration itself is efficient.

Algorithm 1 A framework for brute-force approaches

Enumerate all the plausible assignments of the n_i s

For each assignment n , solve

$$\hat{\ell}(n) = \arg \min_{\ell} \left\| W \left(M(\ell) - \begin{bmatrix} 0 \\ \lambda I \end{bmatrix} n - \begin{bmatrix} r_i \\ \lambda \varphi_i \end{bmatrix} \right) \right\|_2$$

and record the norm of the weighted residual.

Output the solution with the minimal weighted residual.

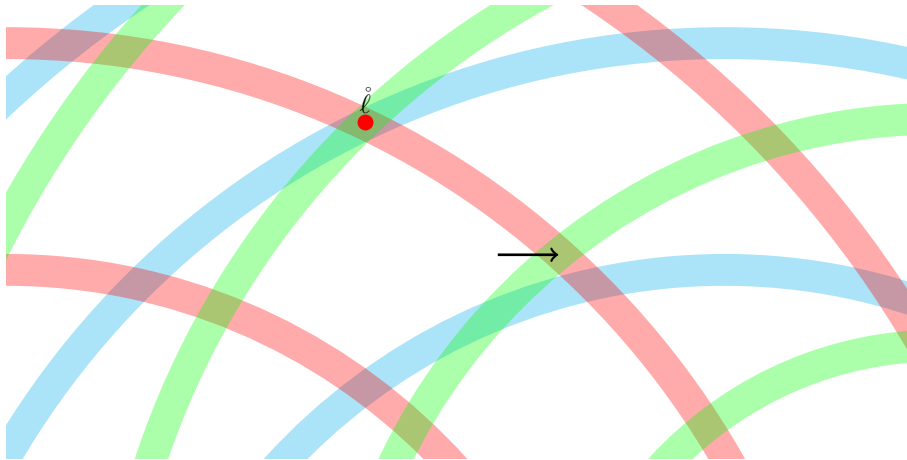


Figure 2: An illustration of 3 families of annuli, depicted in red, green, and cyan. The arrangement has only one cell that is an intersection of one annulus from each family, and in this case it indeed contains the target $\hat{\ell}$, represented by a red dot. The arrangement also contains one almost-intersection, indicated by the arrow.

8.1 Intersections and Near Intersections of Families of Annuli

The constraint

$$\lambda \varphi_i + \lambda n_i = \left\| \hat{\ell} - \rho_i \right\|_2 + \delta_i$$

together with assumed bounds $|\delta_i| \leq D_i$ and $\underline{n}_i \leq n_i \leq \bar{n}_i$ constrain the target $\hat{\ell}$ to an family of concentric annuli (that is, to the union of the annuli in the family). Each annulus in the family contains all the points ℓ whose distance from ρ_i is between $\lambda \varphi_i + \lambda n_{i,j} - D_i$ and $\lambda \varphi_i + \lambda n_{i,j} + D_i$ for some admissible integer $n_{i,j}$. We label this annulus $\mathbb{O}_{i,j}$. The overall constraint for family i is $\hat{\ell} \in \cup_j \mathbb{O}_{i,j}$.

Assuming also that $D_i < \lambda/2$, the annuli in a family are disjoint.

Because all the families constrain the target, it must be lie in the intersection

of the unions of annuli from each family,

$$\mathring{\ell} \in \cap_i \{ \cup_j \mathbb{O}_{i,j} \} .$$

One way to exploit this insight is to create a geometric arrangement of all the annuli and enumerate the cells of the arrangement that are the intersection of one annulus from each family. For intersection cell, we determine the defining integer $n_{i,j}$ of each intersecting annulus $\mathbb{O}_{i,j}$, giving us the vector n of integers for that cell. We solve the continuous least-squares problem induced by n , using a point in the cell as a starting point. One easy way to determine such a point is to compute the intersection of two or three constraints (in 2D or 3D), setting $\delta_i = 0$.

The complexity of the overall arrangement is $O((mE)^2)$ in two dimensions and $O((mE)^3)$ in three.

An effective approximation of this approach, useful in the typical case in which $D_i \ll \lambda$, is to start with two or three families (in 2D or 3D). Let us consider the 2D case for concreteness, denoting the two selected families by i' and i'' . We compute all the intersections of a circle $\lambda\varphi_{i'} + \lambda n_{i',j'} = \left\| \mathring{\ell} - \rho_{i'} \right\|_2$ and a circle $\lambda\varphi_{i''} + \lambda n_{i'',j''} = \left\| \mathring{\ell} - \rho_{i''} \right\|_2$, for all admissible integers $n_{i',j'}$ and $n_{i'',j''}$ (intersections of three spheres in 3D). There are $O(E^2)$ such points, $O(E^3)$ in 3D. Each such point p is in an intersection of an annulus from family i' and an annulus from i'' . The intersection is a parallelogram-type shape with sides that are arcs of circles. We compute the four corners of this shape and determine the maximum distance $\delta_{i',i''}$ from the original intersection point to a corner. We claim that a ball of radius $\delta_{i',i''}$ centered at p covers the intersection of the two annuli. We now iterate over all the other families, computing the nearest annulus from each family to p . If that annulus does not intersect the ball centered at p , we discard the intersection as inadmissible. If one annulus from each family intersects the ball, we declare p to be a *near intersection* and the corresponding vector n of integers as a candidate, and we evaluate the continuous least-squares problem. The complexity of generating the candidate integer vectors is $O(mE^2)$ or $O(mE^3)$.

8.2 Arrangements of Spheres with Integer Radii

For each satellite i we define $\bar{n}_i - \underline{n}_i + 1$ spheres (circles in two dimensions)

$$\lambda n_i = \left\| \ell - \rho_i \right\|_2$$

where $\underline{n}_i \leq n_i \leq \bar{n}_i$. We denote by $E = \max_i \{ \bar{n}_i - \underline{n}_i + 1 \}$ an upper bound on the number of spheres in each family. Every point ℓ in space within the allowed range of distances from ρ_i is contained in exactly one half-open ring defined by two consecutive spheres in the family,

$$\lambda n_i \leq \left\| \ell - \rho_i \right\|_2 < \lambda (n_i + 1) ,$$

where $\underline{n}_i \leq n_i < n_i + 1 \leq \bar{n}_i$. We denote the inner sphere by $n_i = n_i(\ell)$ and we denote the inner sphere for the target is by $\hat{n}_i = n_i(\hat{\ell})$.

The entire collection of at most mE spheres defines a so-called geometric arrangement [9] that decomposes the space into cells bounded by the spheres, faces (parts of the spheres), and vertices (intersections of 3 spheres in 3D and 2 circles in 2D). In the GNSS literature, these cells are called *Voronoi* cells [20] (in the computational-geometry literature the terms Voronoi diagram and Voronoi cell refer to something different; we adopt here the usage from the GNSS literature).

All the points ℓ in a given cell are associated with the same inner spheres $\{n_i(\ell)\}_i$. We refer to this integer vector $n = \{n_i\}$ as the *label* of the cell.

The arrangement structure is important because results in combinatorial geometry show that the number of cells, edges, and vertices in an arrangement of mE spheres in 2D or 3D is only $O((mE)^2)$ or $O((mE)^3)$, respectively, and that these geometric objects can be enumerated in time linear in the number of objects. Therefore, even though there are E^m assignments of valid integers to all the n_i s, only a small set of these assignments are geometrically consistent, and this polynomial-sized subset can be enumerated efficiently.

Therefore, if our phase observations were error free, we could enumerate the cells, determine the label n of each cell, minimize

$$\hat{\ell}(n) = \arg \min_{\ell} \sum_i (\lambda \varphi_i + \lambda n_i - \|\ell - \rho_i\|_2)^2 .$$

for each n , and return the estimate for which the sum of squares is zero.

However, the phase observations do contain errors, so we need to solve instead

$$\hat{\ell}, \hat{n} = \arg \min_{\ell, n} \left\| W \left(M(\ell) - \begin{bmatrix} 0 \\ \lambda I \end{bmatrix} n - \begin{bmatrix} r_i \\ \lambda \varphi_i \end{bmatrix} \right) \right\|_2 .$$

Can we find the minimizers by iterating over all the cells, fixing the integer vector n to the label of each cell, and solve the continuous least squares problem for $\hat{\ell}$ only? Not necessarily. Consider a target $\hat{\ell}$ that is close to its i th outer sphere $\hat{n}_i + 1$ and for which δ_i is larger than the distance between $\hat{\ell}$ and that sphere. We have

$$\lambda \varphi_i + \lambda (\hat{n}_i + 1) = \left\| \hat{\ell} - \rho_i \right\|_2 + \delta_i$$

for some small positive φ_i . There might not be any cell with label

$$\{\hat{n}_1, \dots, \hat{n}_{i-1}, \hat{n}_i + 1, \hat{n}_{i+1}, \dots, \hat{n}_m\} ,$$

as shown in Figure 3, and the constraint

$$\lambda \varphi_i + \lambda \hat{n}_i = \left\| \hat{\ell} - \rho_i \right\|_2 + \delta_i$$

will have a large residual, around λ , not around the magnitude of δ_i .

We conclude that the arrangement of integer-radii spheres allows us to solve problems with no phase errors, but it may fail on problems with phase errors.

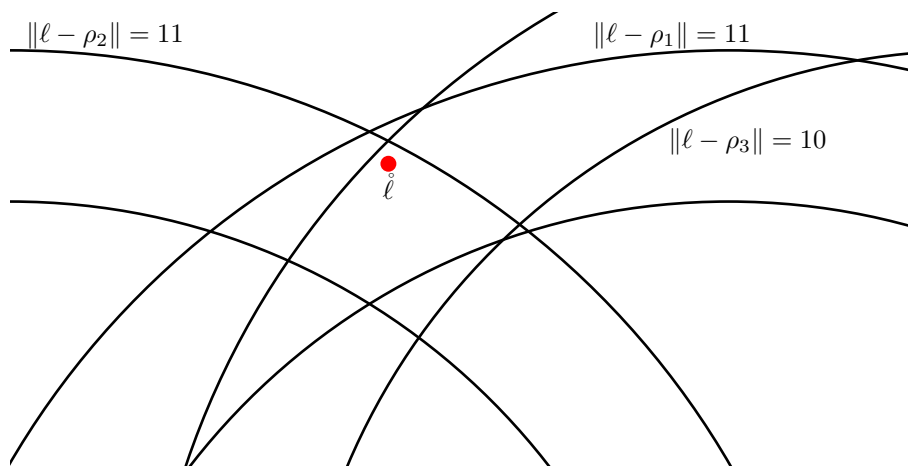


Figure 3: An illustration that demonstrates that the minimizing set of integers might not be the label of any cell in the arrangement. Suppose that $\delta_2 < 0$ and $\delta_3 < 0$, so that $\lambda\varphi_2 + \lambda \cdot 10 = \|\mathring{\ell} - \rho_2\| + \delta_2$ with φ_2 close to 1, and similarly $\lambda\varphi_3 + \lambda \cdot 10 = \|\mathring{\ell} - \rho_3\| + \delta_3$, but that $\delta_3 > 0$ is sufficiently large so that $\lambda\varphi_3 + \lambda \cdot 11 = \|\mathring{\ell} - \rho_2\| + \delta_3$ with $\varphi_3 > 0$ is close to 0. The label of the cell containing $\mathring{\ell}$ is $[10 \ 10 \ 10]$ but the minimizing integer vector is $[11 \ 10 \ 10]$, which is not the label of any cell.

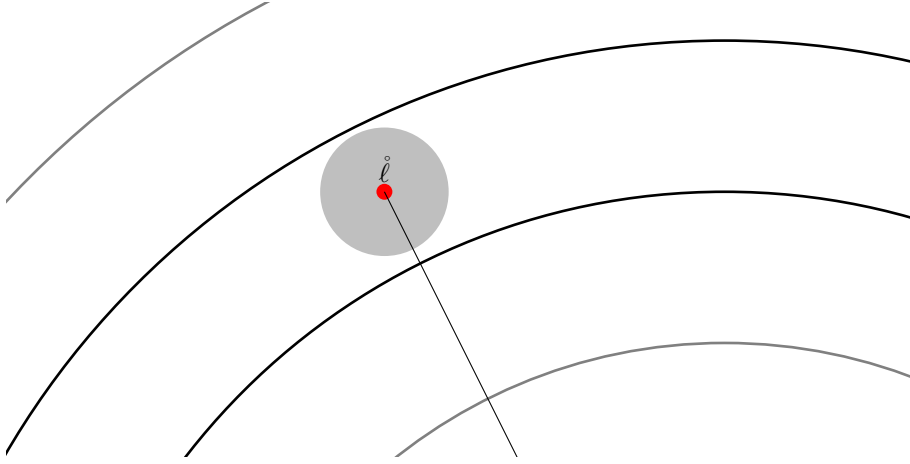


Figure 4: The distance between the target and its inner and outer spheres, bounded from below in Lemma 1. The distance from ρ_i to $\mathring{\ell}$ is $\lambda \mathring{n}_i + \lambda \varphi_i$, to within $\pm \max_i |\delta_i|$, and the radii of the inner and outer spheres are $\lambda \mathring{n}_i - \lambda \varphi_i / 2$ and $\lambda(\mathring{n}_i + 1) - \lambda \varphi_i / 2$.

8.3 Arrangements of Spheres with Shifted Integer Radii

We can address this problem by redefining the arrangement in a way that ensures that the target $\mathring{\ell}$ is far, relative to $\sigma(\delta_i)$, from the faces of the Voronoi cell that contains it. We define the families of spheres

$$\|\ell - \rho_i\|_2 = \lambda n_i - \frac{\lambda}{2} \varphi_i$$

where $\underline{n}_i - 1 \leq n_i \leq \bar{n}_i + 1$. The new definition of the families of spheres induce corresponding assignments of the inner spheres $n_i = n_i(\mathring{\ell})$ and $\mathring{n}_i = n_i(\mathring{\ell})$. The inner spheres define the label of a cell in the same way.

Lemma 1. *Assuming $|\delta_i| < \lambda/2$, the target is in the cell labeled \mathring{n} and distance between the target and the boundary of its cell is at least $\lambda/2 - |\delta_i|$.*

Proof. The radius of the i th inner sphere is $\lambda \mathring{n}_i - \lambda \varphi_i / 2$ and that of the outer sphere is $\lambda(\mathring{n}_i + 1) - \lambda \varphi_i / 2$. The range to the target satisfies the equation

$$\left\| \mathring{\ell} - \rho_i \right\|_2 = \lambda \mathring{n}_i + \lambda \varphi_i - \delta_i .$$

Therefore, the ranges satisfy the inequalities

$$\left\| \mathring{\ell} - \rho_i \right\|_2 = \lambda \mathring{n}_i + \lambda \varphi_i - \delta_i > \lambda \mathring{n}_i - \frac{\lambda}{2} \varphi_i - \delta_i$$

and

$$\left\| \mathring{\ell} - \rho_i \right\|_2 = \lambda \mathring{n}_i + \lambda \varphi_i - \delta_i < \lambda \mathring{n}_i + \lambda \varphi_i - \frac{\lambda}{2} \varphi_i - \delta_i .$$

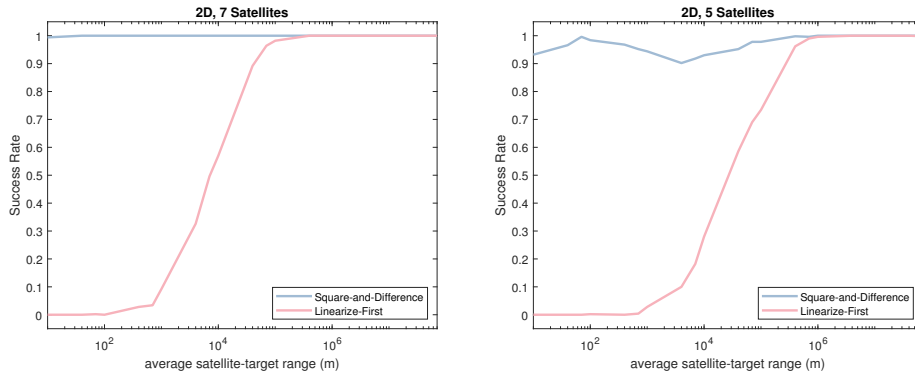


Figure 5: Success rates our new square-and-difference algorithm in two dimensions, compared to that of the linearize-first approach. The graphs plot the success rates for problems with 7 and 5 satellites (left and right).

Therefore, an open ball of radius $\lambda/2 - |\delta_i|$ centered at $\hat{\ell}$ lies outside the ball of radius $\lambda\hat{n}_i - \frac{\lambda}{2}\varphi_i$ centered at ρ_i and inside the ball of radius $\lambda(\hat{n}_i + 1) - \frac{\lambda}{2}\varphi_i$ centered at ρ_i . \square

Once we construct this arrangement, we can enumerate its cells. The vector \hat{n} is among them and is the minimizing vector.

We note that algorithms that correctly enumerate the objects of arrangements of circles and spheres are complex [9]. Currently, there is an implementation of an algorithm that enumerates arrangements of circles [8] but not of spheres.

9 Simulations and Evaluation

We conducted extensive analyses of the algorithms on simulated data. The simulations used the parameters shown in Section 3 unless noted otherwise. We conducted simulations in both 2D and 3D. Simulation data was generated in Python.

We implemented our algorithm in Python and MATLAB. The parts in MATLAB are mostly the integer or discrete least-squares search algorithms, which turned out to be much faster in MATLAB than in Python, probably due to the fact that MATLAB uses a just-in-time-compiler.

We also report on the performance of the LAMBDA approach, which starts with a linearization step and then solves a mixed-integers least-squares problem, which we solve using the MILES software [5], implemented in MATLAB. We refer to this algorithm as the linearization-first algorithm.

Figure 5 compares the success rates of our new square-and-difference algorithm relative to those of MILES on problems in two dimensions with single-epoch data (one observation of each satellite). We define here success as the

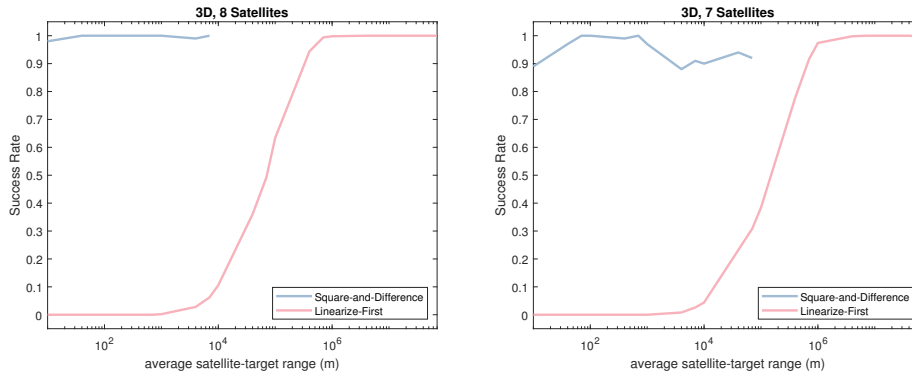


Figure 6: Success rates our new square-and-difference algorithm in three dimensions, compared to that of the linearize-first approach. The graphs plot the success rates for problems with 8 and 7 satellites (left and right).

correct recovery of all the integers. The data shows that with 7 satellites, the square-and-difference algorithm returns correct results down to very short ranges, 40 m. Even at 10 m the algorithm succeeds more than 99% of the time. The linearization-first approach, on the other hand, starts to fail with 7 satellites at ranges of about 40 km, and fails badly at 10 km and below. With only 5 satellites, the square-and-difference algorithm succeeds about 90% of the time or more, but its performance is certainly worse than with 7 satellites. The results with 6 satellites are in between. We stress that failures in the linearization-first approach are caused by the linearization; the linear mixed-integer least-squares solver returns the optimal solution, but the optimal solution of the linearized problem differs from that of the original nonlinear problem.

The results in three dimensions are qualitatively similar, but more satellites are required. Our algorithm gets quite slow in 3D at large ranges (more on that below), so we present its performance at short ranges only. Figure 6 shows with 8 satellites, our algorithm almost always succeeds in 3D at short ranges, whereas MILES fails completely at the same ranges. With only 7 satellites, our algorithm succeeds 90% of the time or more, but its performance is clearly worse than with 8 satellites.

When there are too few constraints, both algorithms fail, as shown in Figure 7. The graphs in the figure show that with 6 satellites both algorithms achieve a success rate of about 80-90% at either short ranges (our algorithm) or long ranges (MILES) but both fail quite badly at other ranges. With only 5 satellites, both algorithms fail miserably.

The two algorithms also behave very differently in terms of their computational efficiency, which determines the running times. Figure 8 presents the running times of the algorithms on 2d problems with 8 satellites at target-satellite ranges of 100 m and 100 km. Running times were measured on a computer with an Intel i7-7500U processor running at 2.7 GHz running Windows and MATLAB

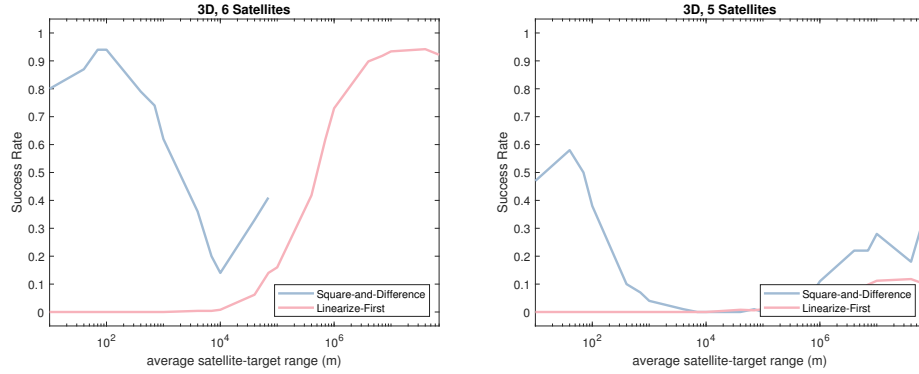


Figure 7: Success rates with too few satellites.

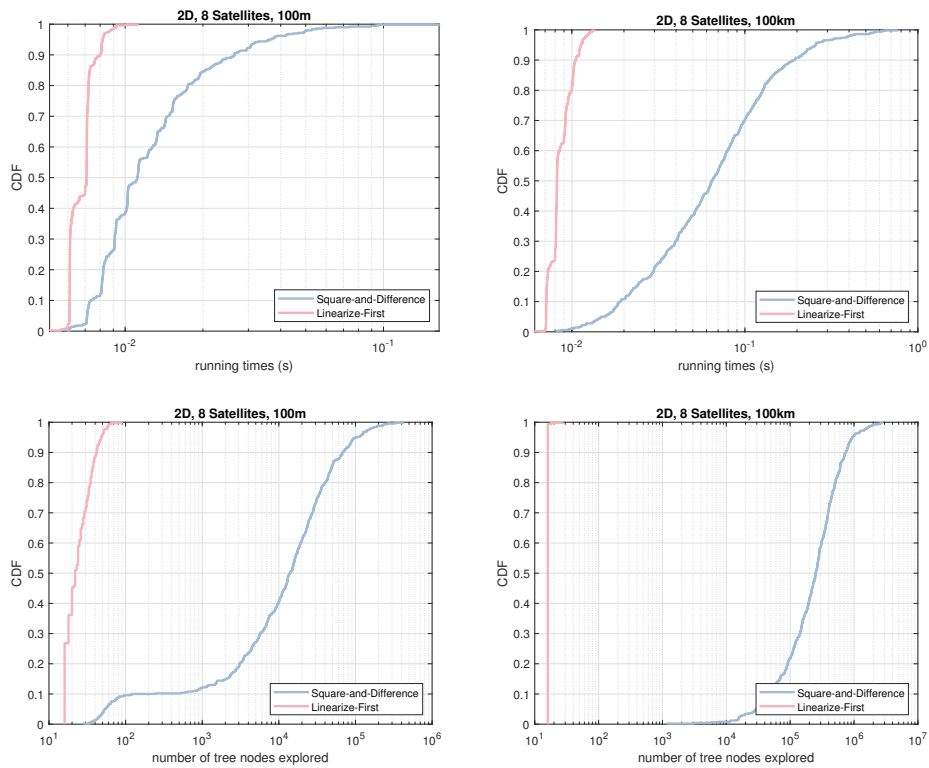


Figure 8: The running times (top row) of the algorithms and the number of tree nodes they explore (bottom row) in two dimensions with 8 satellites, on ranges of 100 m or 100 km between the target and the satellites.

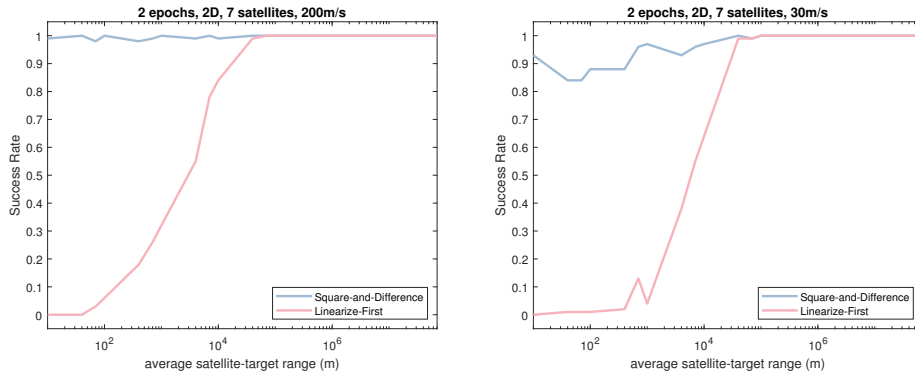


Figure 9: Success rates our new square-and-difference algorithm in three dimensions, compared to that of the linearize-first approach. The graphs plot the success rates for problems with 8 and 7 satellites (left and right).

version 2024a. At short ranges, the running times of the square-and-difference and the linearize-first algorithms are quite similar, with a median running times around 10 ms. Virtually all the runs completed within 100 ms. At ranges of 100 km, in which the linearize-first approach is effective, its running times are short and stable, taking less than 10 ms. The square-and-difference approach is much slower at these large ranges, with a median of over 60 ms and with 10% of the runs taking longer than 200 ms.

The degradation of the performance of the square-and-difference algorithm at high ranges is caused by the $2\delta_i \|\ell - \rho_i\|_2$ term in Equation 5. The algorithm drops this term and compensates with an appropriately-large variance, which forces the search algorithm to consider many more discrete solutions.

The graphs in the bottom row of Figure 8 present the number of nodes that the two algorithms explore in the discrete least-squares search. The data reveals that at short ranges (100 m), the median number of nodes explored is only 40 in the linearize-first approach, versus more than 6,800 in the square-and-difference approach. The wall-clock running times are similar at this range due to the cost of the LLL basis-reduction step, which is used in the linearize-first approach, which searches over the integers, but not in the square-and-difference approach, which searches over squares of shifted integers.

At ranges of 100 km the linearize-first-approach searches even fewer integer assignments, almost always 16, but the square-and-difference approach performs even more assignments, median of more than 143,000. This causes this algorithm an appreciable slowdown relative to shorter ranges.

9.1 Brute-Force Polynomial Approaches

We implemented our two brute-force approaches, the arrangement method and the naive method. The implementation of the naive method is simple. We pick

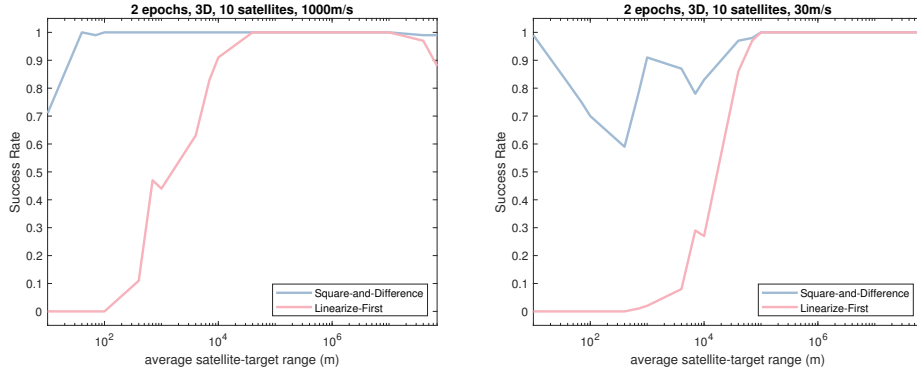


Figure 10: Success rates our new square-and-difference algorithm in three dimensions, compared to that of the linearize-first approach. The graphs plot the success rates for problems with 8 and 7 satellites (left and right).

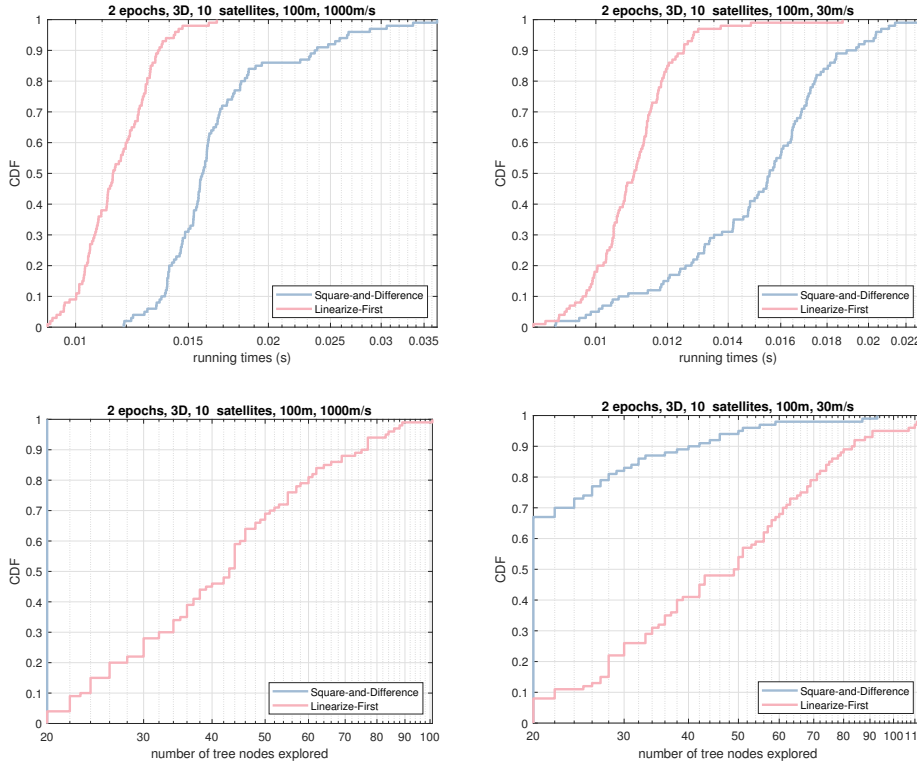


Figure 11: The running times (top row) of the algorithms and the number of tree nodes they explore (bottom row) in two dimensions with 8 satellites, on ranges of 100 m or 100 km between the target and the satellites.

3 arbitrary satellites (2 in two dimensions) and enumerate all the intersections of one sphere for each satellite, for with radii $\lambda n_i + \lambda \varphi_i$ that are up to $\pm 3\sigma(\epsilon_i)$ from r_i . For each intersection consistent with the range observations, we assign the rest of the n_j s and solve the continuous least-squares problem for ℓ , starting from the intersection.

We implemented the arrangement approach, in 2D only, using the SIGAL computational-geometry library [18]. We create an arrangement of all the circles with radii within $\pm 3\sigma(\epsilon_i)$ of the range r_i , for all the satellites simultaneously. We then enumerate the vertices of the arrangement. We identify the two intersecting circles that define the vertex, the corresponding integers, and complete the other integers as in the naive approach.

Both codes are slow, much slower than the other approaches that we proposed, but they are also much more reliable, with negligible failure rates even in difficult cases. Due to their slowness, we only show results for a few interesting ranges, not for a wide spectrum of ranges.

Results will be added to the article soon.

10 Conclusions

We have presented several algorithms for solving location estimation problems involving both noisy range observations (distance measurements) and noisy carrier-phase range observations. The carrier-phase observations measure the remainder of dividing the ranges by a wavelength; they are noisy, but much more accurate than the range observations. These problems represent a simplification of the actual constraints arising in both GNSS and terrestrial settings.

Two algorithms are essentially elimination algorithms. One squares the constraints and then subtract constraints in order to eliminate terms involving non-linear functions of the coordinates. This transforms the problem into a weighted linear least-squares minimization problem, in which some of the unknown parameters are real and some are discrete, but are not integers. We have shown that one of the algorithmic blocks of the LAMBDA approach can solve such problems. The other elimination algorithm uses double differencing, exploiting observations of a moving receivers at two or more times. Both algorithms depend critically on correct weighing of the transformed constraints.

Another family of algorithms project the problem onto the 2- or 3-dimensional space in which the target lies. We enumerate cells in this space that satisfy the carrier-phase constraints, and pick the one on which the overall error is minimized. Because the search is done in 2D or 3D, not in the space of integer ambiguities, the complexity of this algorithm is polynomial, not NP-hard as sometimes claimed [7, Section V].

We demonstrated that our algorithms are efficient and practical.

We plan to extend our algorithms to realistic system model involving ToA observations and carrier-phase observations with nuisance parameters.

References

- [1] Stephen Bancroft. An algebraic solution of the GPS equations. *IEEE Transactions on Aerospace and Electronic Systems*, AES-21(7):56–59, 1985. doi:10.1109/TAES.1985.310538.
- [2] Åke Björck. *Numerical Methods for Least Squares Problems*. SIAM, Philadelphia, PA, USA, 2nd edition, 2024. doi:10.1137/1.9781611977950.
- [3] X.-W. Chang, X. Yang, and T. Zhou. MLAMBDA: a modified LAMBDA method for integer least-squares estimation. *Journal of Geodesy*, 79:552–565, 2005. doi:10.1007/s00190-005-0004-x.
- [4] Xiao-Wen Chang and Christopher C. Paige. An orthogonal transformation algorithm for GPS positioning. *SIAM Journal on Scientific Computing*, 24:1710–1732, 2003.
- [5] Xiao-Wen Chang and Tianyang Zhou. MILES: MATLAB package for solving mixed integer least squares problems. *GPS Solutions*, 11:289–294, 2007. URL: <https://doi.org/10.1007/s10291-007-0063-y>.
- [6] Paul De Jonge and Christian Tiberius. The LAMBDA method for integer ambiguity estimation: implementation aspects. Technical Report LGR-Series number 12, Delft Geodetic Computing Center, Delft University of Technology, 1996.
- [7] Shaoshuai Fan, Wei Ni, Hui Tian, Zhiqian Huang, and Rengui Zeng. Carrier phase-based synchronization and high-accuracy positioning in 5g new radio cellular networks. *IEEE Transactions on Communications*, 70(1):564–577, 2022. doi:10.1109/TCOMM.2021.3119072.
- [8] Efi Fogel, Dan Halperin, and Ron Wein. *CGAL Arrangements and Their Applications—A Step-by-Step Guide*, volume 7 of *Geometry and Computing*. Springer, 2012. doi:10.1007/978-3-642-17283-0.
- [9] Dan Halperin and Micha Sharir. Arrangements. In *Handbook of Discrete and Computational Geometry*, pages 723–762. Chapman and Hall/CRC, 2017.
- [10] A.K. Lenstra, H.W. Lenstra, and L. Lovász. Factoring polynomials with rational coefficients. *Mathematische Annalen*, 261:515–534, 1982. doi:10.1007/BF01457454.
- [11] Franklin T. Luk and Sanzheng Qiao. A pivoted LLL algorithm. *Linear Algebra and its Applications*, 434(11):2296–2307, 2011. doi:<https://doi.org/10.1016/j.laa.2010.04.003>.
- [12] Franklin T. Luk and Daniel M. Tracy. An improved LLL algorithm. *Linear Algebra and its Applications*, 428(11):441–452, 2008. doi:<https://doi.org/10.1016/j.laa.2007.02.029>.

- [13] Jakub Nikonowicz, Aamir Mahmood, Muhammad Ikram Ashraf, Emil Björnson, and Mikael Gidlund. Indoor positioning in 5g-advanced: Challenges and solution toward centimeter-level accuracy with carrier phase enhancements. *IEEE Wireless Communications*, 31(4):268–275, 2024. doi:10.1109/MWC.023.2200633.
- [14] C. P. Schnorr and M. Euchner. Lattice basis reduction: Improved practical algorithms and solving subset sum problems. *Mathematical Programming*, 66:181–199, 1994. doi:10.1007/BF01581144.
- [15] Niilo Sirola. Closed-form algorithms in mobile positioning: Myths and misconceptions. In *Proceedings of the 7th Workshop on Positioning, Navigation, and Communication*, pages 38–44. IEEE, 2010. doi:10.1109/WPNC.2010.5653789.
- [16] P. J. G. Teunissen. The least-squares ambiguity decorrelation adjustment: a method for fast GPS integer ambiguity estimation. *Journal of Geodesy*, 70, 1995. doi:10.1007/BF00863419.
- [17] Peter J. G. Teunissen. Carrier phase integer ambiguity resolution. In Peter J. G. Teunissen and Oliver Montenbruck, editors, *Springer Handbook of Global Navigation Satellite Systems*, pages 661–720. Springer, 2017.
- [18] The CGAL Project. *CGAL User and Reference Manual*, 6.0.1 edition, 2024. <https://www.cgal.org/>.
- [19] Henk Wymeersch, Rouhollah Amiri, and Gonzalo Seco-Granados. Fundamental performance bounds for carrier phase positioning in cellular networks. In *Proceedings of the IEEE Global Communications Conference (GLOBECOM)*, pages 7478–7483, 2023. doi:10.1109/GLOBECOM54140.2023.10437902.
- [20] Peiliang Xu. Voronoi cells, probabilistic bounds, and hypothesis testing in mixed integer linear models. *IEEE Transactions on Information Theory*, 52(7):3122–3138, 2006. doi:10.1109/TIT.2006.876356.
- [21] Peiliang Xu, Elizabeth Cannon, and Gerard Lachapelle. Mixed integer programming for the resolution of GPS carrier phase ambiguities. In *Proceedings of the IUGG General Assembly*, page 12 pages, Boulder, CO, 1995. Also available at <https://arxiv.org/abs/1010.1052>.
- [22] Zhenyu Zhang, Shaoli Kang, and Xiang Zhang. Indoor carrier phase positioning technology based on ofdm system. *Sensors*, 21(20), 2021. doi:10.3390/s21206731.